Received: 2 August 2022 | Revised: 2 May 2023 | Accepted: 2 May 2023

DOI: 10.1111/ppl.13934

ORIGINAL RESEARCH

Physiologia Plantarum

A multifaceted approach to reveal the very-fine root's response of *Fagus sylvatica* seedlings to different drought intensities

Guido Domingo | Candida Vannini | Milena Marsoni | Elena Costantini | Marcella Bracale | Antonino Di Iorio

Department of Biotechnology and Life Science, University of Insubria, Varese, Italy

Correspondence
Antonino Di Iorio, Department of Biotechnology and Life Science, University of Insubria, via Dunant 3, Varese 21100, Italy.
Email: antonino.diiorio@uninsubria.it

Funding information
University of Insubria (FAR)

Edited by K. Noguchi

Abstract

How temperate trees respond to drier summers strongly depends on the drought susceptibility and the starch reserve of the very-fine roots (<0.5 mm in diameter). We performed morphological, physiological, chemical, and proteomic analyses on very-fine roots of *Fagus sylvatica* seedlings grown under moderate- and severe drought conditions. Moreover, to reveal the role of the starch reserves, a girdling approach was adopted to interrupt the flux of photosynthates toward the downstream sinks. Results show a seasonal sigmoidal growth pattern without evident mortality under moderate drought. After the severe-drought period, intact plants showed lower starch concentration and higher growth than those subjected to moderate drought, highlighting that very-fine roots rely on their starch reserves to resume growth. This behavior caused them to die with the onset of autumn, which was not observed under moderate drought. These findings indicated that extreme dry soil conditions are needed for significant root death in beech seedlings and that mortality mechanisms are defined within individual compartments. The girdling treatment showed that the physiological responses of very-fine roots to severe drought stress are critically related to the altered load or the reduced transport velocity of the phloem and that the changes in starch allocation critically alter the distribution of biomass. Proteomic evidence revealed that the phloem flux-dependent response was characterized by the decrease of carbon enzymes and the establishment of mechanisms to avoid the reduction of the osmotic potential. The response independent from the aboveground mainly involved the alteration of primary metabolic processes and cell wall-related enzymes.

1 | INTRODUCTION

Fine root dynamics describe the production, growth, mortality, and decomposition of fine roots, which together contribute to shaping the seasonal pattern in the standing-crop root system (Wang et al., 2019). Fine root dynamics is also widely recognized as a crucial biogeochemical process in forest ecosystems because fine roots represent 22%–33% of the total annual net primary production of trees (Jackson et al., 1997; McCormack et al., 2015) and are an important source of soil carbon as well as a relevant component of the biosphere response to global climate change (Atkin & Tjoelker, 2003).

Since European beech (*Fagus sylvatica* L.) is one of the most widely distributed forest tree species in Europe (Ellenberg, 1988) and the most sensitive to worsening global climate (Cullotta et al., 2015; Geßler et al., 2007; Schall et al., 2012), any adverse effects on its sustainability and regeneration may have great ecological and economic impacts (Fotelli et al., 2009). Previous studies on fine root production of beech forests in southern Europe (Montagnoli et al., 2012, 2014) clearly showed a bimodal seasonal pattern, with two statistically significant peaks followed by periods of necromass production. The maximum seasonal fine root biomass was generally recorded in July, followed by a marked decrease in August. In Mediterranean and temperate regions, July and August coincide with the driest and warmest period of the growing season, making drought one of the main environmental drivers of the midsummer fine root dying event. Soil temperature plays a minor role in this event as it remains optimal (20–22°C) under the canopies of both the Mediterranean *Quercus ilex*-(Montagnoli et al., 2019) and temperate *Fagus sylvatica*-dominated forests (Montagnoli et al., 2014).

Little is known, however, whether a similar fine root seasonal pattern occurs at the seedling stage in the same environment. Espeleta and Eissenstat (1998) reported a higher death rate of adults than that of seedlings in an orchard of *Citrus volkameriana* exposed to progressive soil drying, suggesting higher drought tolerance in seedlings. In growth chamber experiments, the fine root necromass production of *Quercus pubescens* and *Fraxinus ornus* seedlings was stimulated when soil water content (SWC) dropped to values lower than those experienced under natural conditions (Chiatante et al., 2006; Di Iorio et al., 2011). Together, these results suggest that caution should be exercised when extrapolating the responses of seedling roots to those of adult tree roots (Espeleta & Eissenstat, 1998). Thus, seasonal fine root dynamics should be elucidated at the seedling stage, especially considering that drought stress resistance is important for the successful establishment and survival of young seedlings in the field. The present study mainly focused on the very fine root diameter class (<0.5 mm), considered the most reasonable functional root-module for the rapidly cycling portion of the fine root system. In most temperate species, the distal three branching orders perform the primary function of resource uptake and mycorrhizal colonization, and all of them fall within the <0.5 mm diameter class (Guo et al., 2008), making this category the most metabolically active portion compared with the traditional diameter category of <2 mm (Makita et al., 2011). Notably, the recent order-based and functional classification frameworks are sometimes preferred for ecosystems dominated by perennial plants (McCormack et al., 2015).

Drought initially stimulates fine root growth and starch accumulation to a threshold over which starch consumption and mortality rate increase (for a review, see Brunner et al., 2015, Di Iorio et al., 2016). Seedlings of two poplar species (*Populus tremuloides* and *Populus balsamifera*) exhibited reduced accumulation of starch reserves in the root system during the summer (Galvez et al., 2013). The carbon starvation hypothesis predicts that stomatal closure, induced to prevent hydraulic failure under drought conditions, diminishes the photosynthetic uptake of carbon, and the plant starves as a result of continued metabolic demand for nonstructural carbohydrates (NSCs), that is, soluble sugars (SS) and starch (McDowell et al., 2008). Other mechanisms involved in drought-induced fine root mortality and tree mortality generally include hydraulic failure and phloem transport disruption, which impedes carbon translocation to the downstream sinks (Brunner et al., 2015; Hartmann et al., 2013, 2018). Therefore, drought-induced death of fine, and especially very fine, roots can reasonably involve both direct and indirect damage (the former due to cortical lacunae formation and root shrinkage (Cuneo et al., 2016), and the latter due to an imbalance between carbon uptake and loss), resulting in negative carbon balance (Brunner et al., 2015, Hartmann et al., 2013, 2018).

The respiration rate is usually considered an index of root metabolic activity (Polverigiani et al., 2011). Root growth is strongly associated with respiration costs, usually partitioned among the functional components of construction, maintenance, and ion uptake (Bouma et al., 1997; Makita et al., 2009). In response to soil drying, respiration rate shows no marked change at low soil temperatures (10°C) but declines at moderate to high temperatures (20–30°C; Di Iorio et al., 2016; Huang et al., 2005). Moreover, respiration rate shows a direct correlation with SS concentration and an indirect correlation with starch concentration (Di Iorio et al., 2016; Jia et al., 2013; Lipp & Andersen, 2003).

Beyond serving the nutritional and energy requirements of plants, NSCs also play regulatory roles in controlling gene expression in leaves, bark, and roots (Li et al., 2003); however, little is known about these molecular mechanisms at the fine and very fine root levels. Nevertheless, comparative proteomics has been widely used to unravel the mechanisms underlying the root response to drought stress (Gupta et al., 2020; Li et al., 2020, 2022; Liu et al., 2015, 2019). A combination of physiological, morphological, and proteomic approaches has proven useful for an in-depth investigation of the different responses of fine roots to water deficit (Geilfus et al., 2017; Xiao et al., 2020). Proteomics studies are very informative since proteins are the functional molecules in cells and provide a more accurate representation of the plant phenotype than nucleic acids (Vogel & Marcotte, 2012).

To address the contribution of the impeded carbon translocation to the fine root response to severe drought (SD) conditions, a carbon-supply limiting approach via the ringbarking (girdling) technique was applied to 2-year-old beech (*F. sylvatica*) seedlings transplanted under seminatural conditions. This treatment was performed in July, which marks the beginning of the driest period of the growing season. Girdling instantaneously terminates the flux of photosynthates from the shoot to roots through the phloem but enables water and nutrient transport in the reverse direction through the xylem. Furthermore, girdling triggers the depletion of NSCs below the girdling zone (Oberhuber et al., 2017).

The present experiment was designed to impede phloem transport in the core summer period, when the water deficit increases, while continuously monitoring changes in relevant morphological, physiological, and molecular processes, including (1) whole-plant growth and very fine root morphology, (2) whole-plant NSC (starch

and SS) content, (3) very fine root respiration, and (4) proteome remodeling. Specific objectives of this study were as follows: (a) to test whether the seasonal pattern of very fine seedling roots differs from that of very fine adult beech tree roots usually reported in the literature; (b) to determine whether carbon pools decrease under SD stress and whether this reduction induces very fine root death; (c) to investigate whether storage pools are affected similarly in all woody compartments (stem and taproot, the main large and dominant root); and (d) to reveal the molecular mechanisms underlying the drought stress response of very fine roots using a proteomics approach. Proteomic investigations were performed only on very fine root samples collected in August, after the fine roots of adult trees, as previously stated, had experienced the driest soil in the growing season and had shown a marked decrease in biomass.

2 | MATERIALS AND METHODS

2.1 | Plant material and growing conditions

In February 2015, 76 one-year-old uniformly sized (top bud 25–30 cm high) dormant *F. sylvatica* seedlings from a northern Italy seed source (provided by the ERSAF nursery in Curno, Bergamo, Italy) were transplanted into 9.5 L (24 × 24 cm) plastic pots. To better focus on the newly emitted roots, the root-soil cylindrical clot of nursery origin was positioned within a 1.50 mm mesh cylinder approximately 7 cm diameter and 20 cm high (Figure S1) before being potted. The buried pots approach was adopted to provide a uniform edaphic environment, mimic the diurnal and seasonal pattern of soil temperature and facilitate whole-root system recovery. To this aim, the bottom of the pot was replaced by a 40 μm (0.4 mm) mesh-net grafted to the pot wall. The mesh size was small enough to avoid the out-of-pot growth of the roots and to best reduce pot artifact by improving water drainage. Pots were filled with a mixture of mineral soil, sand, and humus manure (50:40:10) and buried outdoors into the ground (Figure S2). A commercial slow-release NPK (2:1:1) fertilizer (≈60 g per pot) was added to the mixture.

Recovery from dormancy and complete leaf expansion occurred during the April establishment period when all saplings were watered on an as-needed basis to field capacity. From early May onwards, all plots received natural precipitation in 2015 except those subjected to SD stress during July and August.

2.2 | Experimental design

The experiment started in early May 2015 and lasted 1 year, pausing during the winter dormancy. Samplings were performed monthly during the 2015 growing season, with exactly six sampling points between early May and early November, plus a seventh in early May 2016. The summer of 2015 was particularly warm and dry, with only 50 mm of rainfall in 55 days (middle of June–middle of August) (Figure S3a). These conditions made it possible to fix the onset of moderate drought (MD) at the beginning of June when the volumetric SWC dropped to 15% (Figure S3b). Starting on 6 July 2015, pots for SD treatment were excluded from any precipitation with a manual transparent rain-out plastic shelter (1.5 m height) promptly stretched by hand and tailored to cover the SD plants in case of rainy events until mid-August 2015. MD pots were maintained uncovered under natural summer conditions and watered when the volumetric SWC dropped below 15%, the lower limit observed in field sites in the Italian Pre-Alps (Montagnoli et al., 2014). MD pots have been considered this experiment's "natural" control condition.

After the third sampling on 6 July, plants were subjected to the girdling processing (Figure S2) so that the experimental design resulted in four water + girdling treatment combinations (two water levels × two girdling levels) in a completely randomized factorial design as follows: "natural" MD without girdling (NG-MD; control), "natural" MD with girdling (G-MD), induced severe drought without girdling (NG-SD), induced severe drought with girdling (G-SD). As 4 replicates for each combination of treatments were harvested at each sampling point, 16 replicates were assigned to each combination of treatments (4 replicates × 4 sampling points), totalling 64 seedlings (16 replicates × 4 treatments), and 76 including the first three samplings.

Drought: "natural" MD (natural summer condition, with watering when the volumetric SWC dropped below 15%) and induced SD (plants were excluded from any precipitation from 6 July to mid-August; the minimum water content of the soil recorded was 9.1%).

Girdling (annulation): the bark of seedlings has been removed (G, girdled) at the level of the stem to block the flow of photoassimilates; using a scalpel, the superficial part of the cortex was removed, taking care not to damage the cambial area. The cut was made 5–6 cm from the collar and coated with lanolin, a waterproofing material to protect the exposed tissues from dehydration and the action of pathogens.

2.3 | Morphological and biomass measurements

Four replicates for each combination of treatments were harvested at each sampling point. For each plant, new roots outside the mesh cylinder were carefully freed from soil by brushing. During operation, exposed roots were kept moist by a nozzle sprayer. After the detection and removal of dead roots, if any, depending on their dark brown color, texture and shrunk shape, all new live fine roots were excised and placed in water-filled basins; remaining soil particles were carefully removed using soft paint brushes. The roots were scanned immersed in water at a resolution of 400 dpi with a calibrated flatbed scanner coupled to a lighting system (Expression 10000 XL, Epson America Inc.) for image acquisition. The resulting images were analyzed with Win-RHIZO Pro 2007d software (Regent Instruments Canada Inc.) to group with high accuracy, the root mat/fragments in three diameter classes, namely very-fine (Ø ≤ 0.5 mm), fine (0.5 < Ø ≤ 2 mm); no root fragments larger than 2 mm in diameter were considered in this study. The pertinent root length, volume (cm^3), and average diameter measurements were performed.

Upon image analysis, very-fine and fine roots were weighed separately, and two sub-samples of 250–300 mg and 700–750 mg fresh weight of very-fine roots alone were selected for respiration and proteomics measurements, respectively. Successively, respiration and remaining samples were pooled and oven-dried at 70°C for 3–5 days for dry mass measurements. The dry mass estimation of proteomic samples was based on the mean water content (%) measured in the pooled samples. To evaluate biomass allocation, plants were divided into shoots, leaves, taproots, and the remaining laterals inside the mesh cylinder and weighed after oven-drying to constant weight at 70°C. Then, dried very-fine and fine roots, as well as taproot and shoot samples, were separately ground in a Wiley mill and stored at −20°C for SS and starch analyses.

2.4 | Root respiration

On each sampling day, very-fine root respiration was measured for each sapling, respectively. Each root sample (250–300 mg fresh weight) coming from image analysis was quickly wiped from excessive free surface water on blotting paper and then immediately inserted in a specifically designed respiration cuvette (16 cm^3 volume; Di Iorio et al., 2016) connected to an infrared gas analyzer (IRGA, EGM-3, PP Systems). For roots coming from drought-treated plants rewetted for scanning operation, previous works (Burton et al., 1996; Palta & Nobel, 1989; Vartanian & Chauveau, 1986) highlight how rinsed roots return to normal respiration rates only several hours (24–36 h) after rewetting. Thus, no bias occurred in respiration measurements within the 2 h of laboratory procedure from sample collection.

Cuvette was maintained vertically, temporarily sealed at both ends and placed in a water bath to maintain root samples at the experimental ST. The IRGA and cuvette were configured in an open system with two airflow lines of 300 mL min^{-1}, one for the blank and one for the cuvette. The inlet CO_2 concentration was set at ≈0 μL L^{-1}. Measurements consisted of 1 min incubation interval alternating with 1 min continuous flow interval for a total of eight incubation measurements in 17–18 min (three 35 s auto zero intervals every 4 min). Only the last four measurements were accepted for statistical analysis as previous tests with further measurement cycles (40 min) did not significantly change the CO_2 concentration recorded after 8 min.

Root respiration rate was determined as the difference between the maximum concentration of CO_2 leaving (after incubation) and entering (before incubation, 0 μL L^{-1}) the cuvette on a 60 s basis. Measurements also accounted for CO_2 produced by rhizosphere microbial respiration, as it was assumed to be plant-derived C sources (Wiant, 1967). After the measurement, the root sample was removed from the cuvette and oven-dried for successive NSC measurements. Root respiration rate (R_r) was expressed on a dry mass basis (nmol CO_2 g^{-1} s^{-1}):

$$R_r = \left(\frac{C_{CO_2}(\max) - C_{CO_2}(t_i)}{\Delta t}\right)\frac{V_s}{V_{air}}\frac{273.15}{273.15+T}\frac{10^3}{DW}$$

where C_{CO_2} (max) is the max CO_2 concentration (μL L^{-1}) after 1 min incubation and C_{CO_2} (t_i) at start time (0 μL L^{-1}), Δt is the time interval (60 s), V_s is the volume of respiration cuvette (0.016 L), V_{air} is the standard gas volume (22.414 L mol^{-1}), T is soil temperature (°C), and DW is dry mass of the root sample (g).

2.5 | NSCs sampling and analysis

SS and starch content of all plant tissues were determined following Landhäusser et al. (2018). Samples were collected 3–4 cm above the girdled zone and below the root collar for stem and taproot NSC measurements. Dried samples were ground in a Wiley Mill to pass through a 40-mesh screen. SS were then extracted in 80% ethanol, and their content was determined spectrophotometrically via a phenol–sulfuric acid assay. After extraction, starch in the remaining pellet was digested with α-amylase and amyloglucosidase (Sigma-Aldrich), and the resulting glucose content was determined spectrophotometrically using glucose oxidase/peroxidase-o-dianisidine solution and converted to starch equivalent. Sugar and starch concentrations were calculated as a percent of the sample dry weight. NSC concentrations are the sum of starch and SS. The Supporting Information (procedures for soluble sugars and starch quantifications) provides a complete description of the protocols.

2.6 | Protein extraction and digestion

Total proteins were extracted from lyophilized samples of very-fine roots (≈ 150 mg), following the phenolic extraction protocol described in (Vannini et al., 2021). The extracted proteins were quantified with 2-D Quant-kit (Amersham) and digested with trypsin via the filter aided sample preparation (FASP) technique as described by Paradiso et al. (2020). A complete description of protein extraction and digestion can be found in the supplemental material. Total peptide concentrations, adequate for LC–MS/MS analysis (500 ng), were estimated spectrophotometrically, assuming that a solution of proteins with a concentration of 1 mg mL^{-1} determines an absorbance of 1.1 at 280 nm.

2.7 | LC–MS/MS analysis and elaboration of raw data

The peptides were analyzed in a QExactive mass spectrometer as described in the literature (Vannini et al., 2021). Raw data were searched with the MaxQuant program (v.1.5.3.3, http://www.coxdocs.org/doku.php?id=maxquant:start) against the *Populus trichocarpa* database (by www.plantgdb.org/PtGDB). The search criteria were as follows: two missed cleavages, fixed modification of cysteine (carbamidomethylation), variable modifications of methionine (oxidation) and phosphorylation on serine, threonine and tyrosine, minimum peptide length of six amino acids, precursor mass tolerance 4.5 ppm

for the main search. Label free quantification (LFQ), "match between runs" (time window of 0.7 min) and target-decoy search strategy (revert mode) options were enabled. A false discovery rate (FDR) of 1% was accepted for peptide and protein identification, respectively. Incorrect identifications ("Reverse," "One site," and "Contaminant" hits) and not consistent identifications were filtered out from MaxQuant output files. Only protein groups detected in at least two of the three biological replicates in almost one analytical group were considered to assess significant changes. Missing values were estimated by using an in-house tool (Vannini et al., 2019). The filtered data were processed with the Perseus software platform (http://www.perseus-framework.org). Log2 transformed LFQ intensities of protein groups intensities were centered by subtracting the median of the entire set of protein groups LFQ intensities per sample (column). Hierarchical clustering analysis was carried out using the Perseus software and default parameters. The mass spectrometry proteomics data were deposited in the ProteomeXchange Consortium via the PRIDE (Perez-Riverol et al., 2019) partner repository with the dataset identifier PXD028395.

2.8 | Statistical analysis

A factorial experiment with a completely randomized design was set up with two main factors: water availability and girdling disturbance. The main and interaction effects of time, drought intensity and girdling on root biomass, respiration rate and several morphological and chemical traits were tested with a three-way ANOVA using the General Linear Model (SPSS Inc.). This analysis considered only the last four of seven samplings because the girdling event was applied at the third sampling. All interactions were initially included in the model, the non-significant ones being stepwise excluded. All data were tested with the Kolmogorov–Smirnov test for normality and the Levene test for the homoscedasticity assumption. The fine root mass met these requirements after square-root transformation. For each variable, one-way ANOVA and the least significant difference pairwise multiple comparison test were performed among treatment combinations within each sampling day and among sampling days within each treatment combination. Redundancy analysis (RDA) was performed on all standardized data to detect the pattern of association between the very-fine root morphological (length, dry mass) and physio-chemical (specific root respiration, starch, and SS) response variables and the soil temperature (ST) and SWC explanatory variables under different drought and girdling conditions (software SYN-TAX 2000, Podani).

Protein fold change (FC) ratio, expressed as Log2FC, is defined as the Log2 of protein abundance in one biological condition minus Log2 protein abundance in another biological condition (e.g. NG-MD vs. NG-SD, NG vs. G, G-MD vs G-SD). Log2 transformed, centered, and/or normalized LFQ data were subjected to two-way ANOVA tests using an FDR cut-off of 0.05.

The Perseus software was also used for principal component analysis (PCA), plot scattering, and hierarchical clustering analysis to assess the quality of our datasets.

2.9 | Downstream bioinformatic analysis

MaxQuant output file hits were represented by a group of proteins (group of IDs) sharing the same set or a subset of peptides of the best matching leading protein. For bioinformatics analysis, only the leading protein was considered. To be able to use some bioinformatic tools (i.e., ShinyGO) available only for *Arabidopsis thaliana*, *F. sylvatica* proteins were compared with those of *A. thaliana*. A local BLAST on WINDOWS 10 operating system was performed using the *A. thaliana* blastset TAIR10 (version 2012-05-07) downloaded from Tair (http://www.arabidopsis.org/index.jsp). The enrichment analysis was performed using ShinyGO v0.61 (Ge et al., 2020) with a P-value cutoff (FDR) of 0.05.

3 | RESULTS

3.1 | Time-course of morphological, physiological, and NSCs responses to soil drying and girdling

The summer of 2015 was particularly warm and dry. Precipitation and air temperature patterns highlighted a MD period from mid-June to mid-August, with 50 mm in 55 days of rainfall and a mean maximum air temperature of 31 ± 2.96°C (Figure S3a). Volumetric SWC for MD treatments was 12.5 ± 1.3% in July and August, whereas it further dropped to 9.5 ± 1.7% under SD conditions (Figure S3b). The highest soil temperature at 5 cm soil depth was 26.5 ± 0.7°C in July for, decreasing in August to 20–21°C (Figure S3c). As the temperature of the top soil layer rises faster in dry than in wet soils (Abu-Hamdeh & Reeder, 2000), it is worth noting that the values in the severe droughted soils were, on average, ~2° higher than those in moderate droughted.

At the morphological level, drought and girdling significantly affected the very-fine root length ($p = 0.031$), and the negative effect of girdling significantly intensified with time (significant TxG interaction at $p < 0.001$, Table 1). Girdling also affected the dry mass in a similar way as well as the decrease in time (significant TxG interaction at $p < 0.001$, Table 1); on the other hand, the course of the season (time) significantly affected only the dry mass ($p = 0.011$, Table 1). Very-fine roots of moderately stressed intact plants (NG-MD), considered as control, showed constant growth until August to stop with the end of the growing season (Figure 1). This was particularly evident for the length rather than the dry mass, whose growth rate remained almost constant. Severe drought (NG-SD) further stimulated the growth until the end of September, with the dry mass rather than length mean value significantly higher than control, for decreasing in 1 month with the incipient fall; both dry mass and length increased again in the following growing season.

Very-fine roots of girdled plants, independently from the drought intensity, showed an increase in length rather than mass during the 42 days following the girdling treatment markedly higher than that of intact plants, decreasing progressively until November.

TABLE 1 *F* and *p* values of ANOVA (General Linear Model) for the effects of time, girdling, and drought on morphological and physiological very-fine root traits.

Trait		Time	Girdling	Drought	$T \times G$	$T \times D$	$G \times D$
Root length (cm)	*F*	2.653	16.668	5.288	8.926	-	-
	p	*0.074*	***<0.001***	***0.031***	***<0.001***	-	-
Root dry weight (g)	*F*	4.773	41.210	3.637	9.366	-	-
	p	***0.011***	***<0.001***	*0.071*	***<0.001***	-	-
Respiration (nmol CO_2 g^{-1} s^{-1})	*F*	0.491	55.607	1.354	-	-	-
	p	*0.692*	***<0.001***	*0.255*	-	-	-
Starch (%)	*F*	5.532	29.979	0.359	3.601	-	-
	p	***0.005***	***<0.001***	*0.555*	***0.029***	-	-
SS (%)	*F*	2.408	9.433	1.050	-	-	-
	p	*0.083*	***0.005***	*0.315*	-	-	-

Note: Nonsignificant interactions effects were excluded from the model (-). Italics refer to *p* values; boldface *p* values are significant at a probability level of $p < 0.05$.

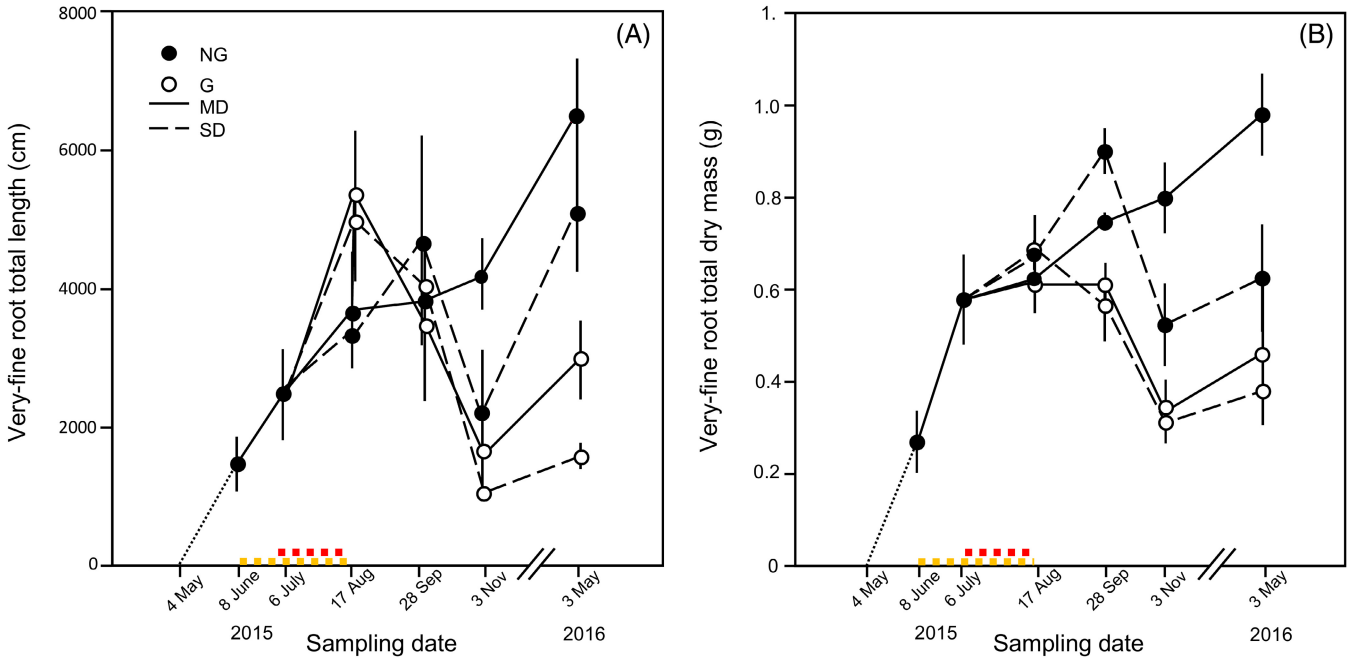

FIGURE 1 Seasonal pattern of very-fine root total length (A) and dry mass (B) for two-years old *Fagus sylvatica* seedlings under four girdling/drought treatment combinations (see Section 2). Continuous (—) and dashed (– – –) lines indicate moderate-drought and severe-drought conditions, respectively; filled and empty circles indicate intact and girdled plants, respectively. Symbols refers to each sampling date and represent the means of 4 replicates ± 1SE. Colored strips indicate the duration and intensity of the drought treatments: dark-yellow for moderate-drought, red for severe-drought.

In contrast, relevant were the root respiration rate changes observed during the examined period (Figure 2A). Under MD conditions, the respiration rate fluctuated around 6.5 nmol g^{-1} s^{-1}, with the lowest mean value in July when the soil temperature was as high as 26.5°C and in November when it was as low as 10°C (Figure 2A). In response to the same soil temperatures, severely droughted plants reduced their respiration rate, although a slight increase was observed through September with values similar to the control. Girdling treatment significantly reduced the respiration rate ($p < 0.001$, Table 1), particularly in severe-stressed plants.

Starch concentration in NG-MD very-fine roots showed a bell-shaped pattern from May to May throughout the growing season (Figure 2B). It slightly decreased between June and July but did not change in intact plants till September, after which it declined to start values in May of the following year. In NG-SD plants, after a slight increase, starch concentration anticipated the decrease starting from August, and then the pattern was in line with that of control. A strong significant decrease was observed in girdled individuals ($p < 0.001$, Table 1) independently from the drought intensity, and this decrease significantly increased with time (significant TxG interaction at $p = 0.029$, Table 1).

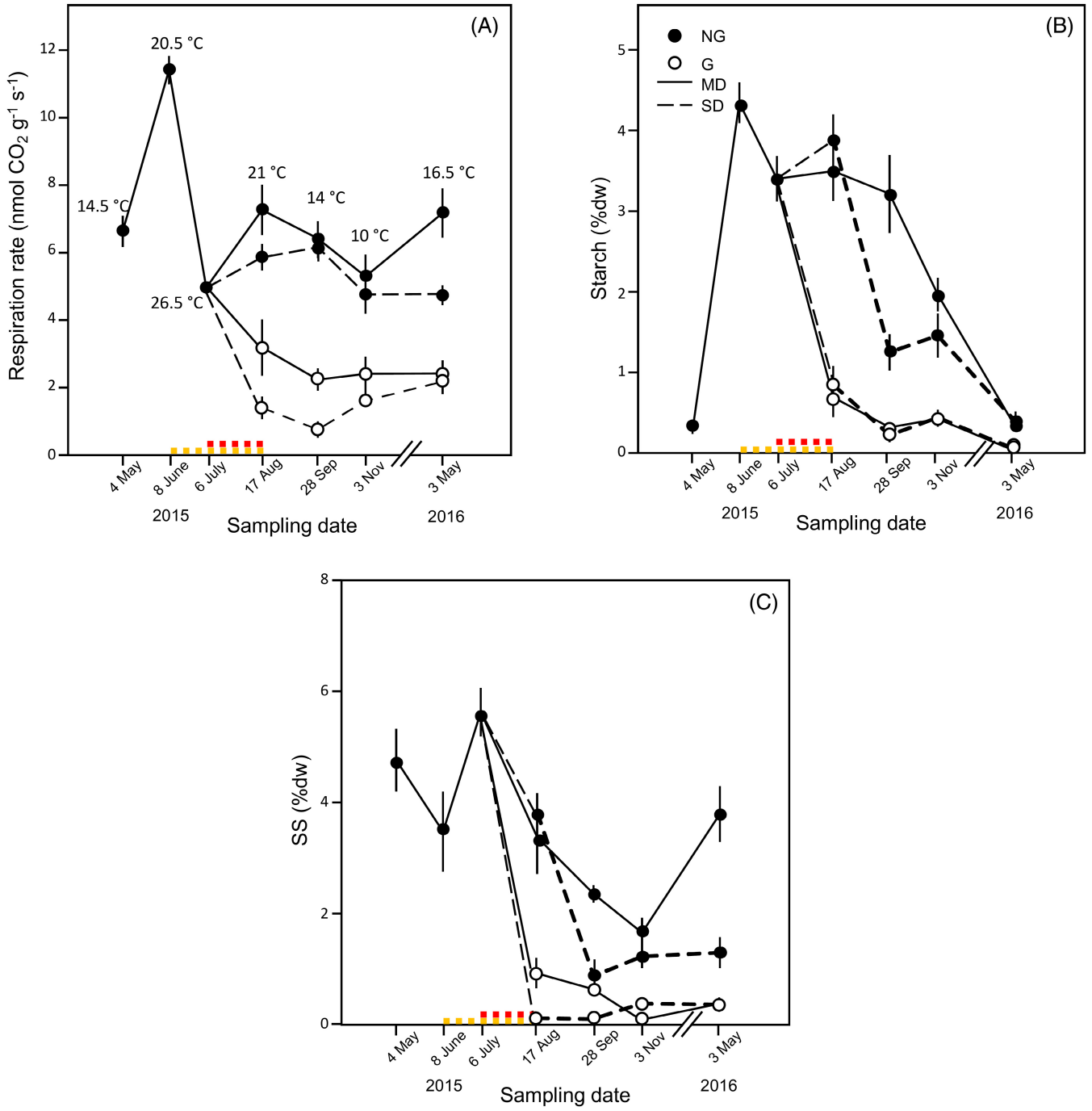

FIGURE 2 Seasonal patterns of respiration rate (A), starch (B), and soluble-sugars (C) concentrations for very-fine roots of 2-years old *Fagus sylvatica* seedlings under four girdling/drought treatment combinations (see Section 2). Continuous (—) and dashed (– – –) lines indicate moderate-drought and severe-drought conditions, respectively; filled and empty circles indicate intact and girdled plants, respectively. Symbols refers to each sampling date and represent the means of 4 replicates ± 1SE. Colored strips indicate the duration and intensity of the drought treatments: dark-yellow for moderate-drought, red for severe-drought. For the respiration rate panel only, numbers refer to the soil temperatures averaged among treatments at each sampling date.

SS showed a pattern different from that of starch (Figure 2C), with a significant decrease starting in July to increase again at the beginning of the new growing season. As for starch, girdled plants showed a drastic decrease ($p = 0.005$, Table 1) immediately after the girdling treatment and did not increase again at the beginning of the new growing season.

By analyzing the pattern of association between the very-fine root morphological and physio-chemical traits under different drought (SWC and ST) and girdling conditions (Figure 3), the first axis of the RDA explained 87.81% of the total variance, with all the morphological and chemical variables grouped toward large positive loadings, except for the specific respiration rate; they were positively and

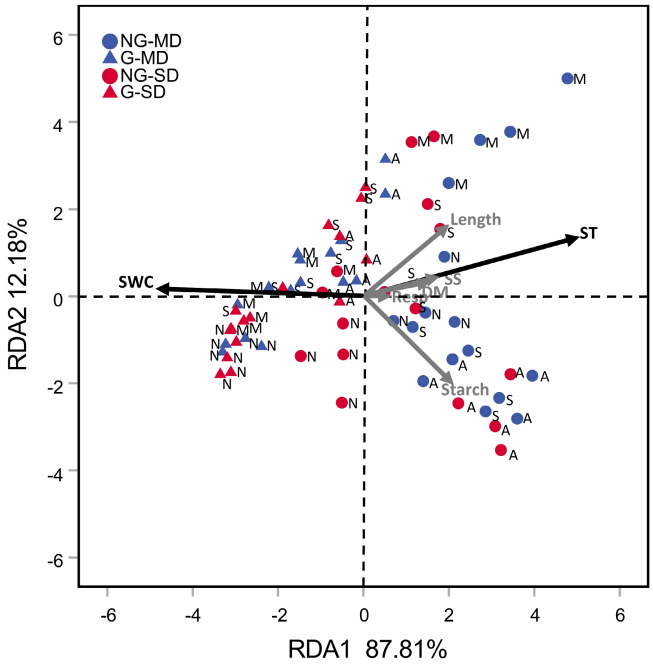

FIGURE 3 Redundancy analysis of very-fine root morphological and physio-chemical traits under different drought (SWC and ST) and girdling conditions. Red, severe-drought; blue, moderate-drought; circle, intact; triangle, girdled; Length, total length; DM, dry mass; SS, soluble sugar; Starch, starch; Resp, specific respiration rate; ST, soil temperature; SWC, soil water content. A, S, N and M refer to months August, September, November 2015, and May 2016, respectively.

negatively correlated with ST and SWC, respectively. Intact (NG) and girdled (G) plants were clearly separated on the first axis, with the former closely associated with all the response variables investigated. Length and starch concentration accounted for most of the 12.18% total variance of the second axis, with August and September severe droughted samples associated with starch and length, respectively.

For the other organs investigated, the taproot starch concentration and SS showed the same patterns as very-fine roots, although the magnitude was four-fold and two-fold higher, respectively (Figure S4a,b). Unlike the very-fine roots, the mean values of severe-drought stressed plants (NG-SD) remained the highest throughout the rest of the season and in the new one.

Above the girdle, as expected, stem starch concentration was higher in girdled (G-MD) than intact plants (NG-SD) if moderately droughted (Figure S4c). No differences occurred between severe-droughted treatments, although after July, the mean values remained lower than moderately droughted individuals. No clear trend emerged for SS concentration sampled above the girdle except for the NG-MD treatment, whose pattern was similar to taproot and very-fine roots (Figure S4d).

3.2 | SD- and girdling strongly affect root proteomic profiles

The proteomic analysis was conducted on very fine roots collected in coincidence of the driest period of the growing season, 42 days since the girdling treatment. A total of 996 proteins were identified: after the filtering process, 422 were quantified in all samples (data not shown). Principal component analysis (PCA) showed that biological replicates were plotted very closely in the PCA space, indicating a good correlation between replicates (Figure S5). The severe drought-stressed samples (NG-SD and G-SD) were separated in PC1 from MD-stressed samples (NG-MD and G-MD), and this accounted for 57.5% of the total variation, indicating that water stress strongly affected the proteome (Figure S5).

The selected 422 proteins were subjected to a two-way ANOVA test (Table S1) to identify the differentially abundant proteins (DAPs) expressed under the different treatment combinations considered with respect to the control condition (NG-MD). For a deeper investigation, DAPs were clustered based on the modulation of their expression. Figure 4 shows some of the protein profiles obtained.

Cluster 1A and 1B consisted of proteins up- and downregulated, respectively, in response to SD, regardless of the girdling treatment (Figure 4, Table S2). Carbon metabolism, tricarboxylic acid cycle (TCA), glycolysis and arginine biosynthesis are the most represented biological processes involving proteins belonging to cluster 1A (Table S5). SD stress decreased the levels of three enzymes involved in amino acid metabolism, including two aminotransferases (POPTR_0018s08910.1), a glutamate dehydrogenase (POPTR_0019s05050.1), and three enzymes related to arginine biosynthesis and degradation such as arginase (POPTR_0002s14720.1), urease (POPTR_0002s24520.2), and ornithine carbamoyltransferase (POPTR_0005s25100.1; Table 2, Table S2). Moreover, SD also decreased the concentration of POPTR_0015s07550.1, a protein similar to the mitochondrial delta-1-pyrroline-5-carboxylate dehydrogenase 12A1, which is involved in proline degradation.

Among DAPs involved in protein metabolism, changes in the abundance in some proteasome subunits (POPTR_0005s25080.1, POPTR_0006s14260.1, POPTR_0001s16310.1, POPTR_0014s18530.1, SUMO 2; POPTR_0014s15650.1) were also observed: among them the 26S proteasome subunit RPT2a (POPTR_0014s18530.1), which controls root meristematic activity (Ueda et al., 2004; Table 2, Table S2).

Among the DAPs of cluster 1B, POPTR_0009s02050.1, similar to tetraspanin 3 (TET3), which is involved in the regulation of cell differentiation (Wang et al., 2015), and POPTR_0009s11920.1, a homolog of the glycine-rich RNA-binding protein GRP8 in Arabidopsis, involved in post-transcriptional regulation of root hair cell fate (Foley et al., 2017), were increased by SD.

Overall, these data indicate a general decrease of proteins involved in the carbon metabolism as the drought progressed in fine roots, independently from the interruption of resource fuelling from aboveground.

Interestingly, two-way ANOVA analysis revealed 193 proteins with a regulation dependent on the interaction between drought intensities and girdling treatment (Table S1). Among these, cluster 2A grouped proteins whose abundance decreases both in NG plants if severely stressed (NG-SD) and in all girdled plants (G-MD and G-SD), with respect to moderately stressed intact plants (NG-MD) (Figure 4, Table S3). These results indicate that a similar response to drought

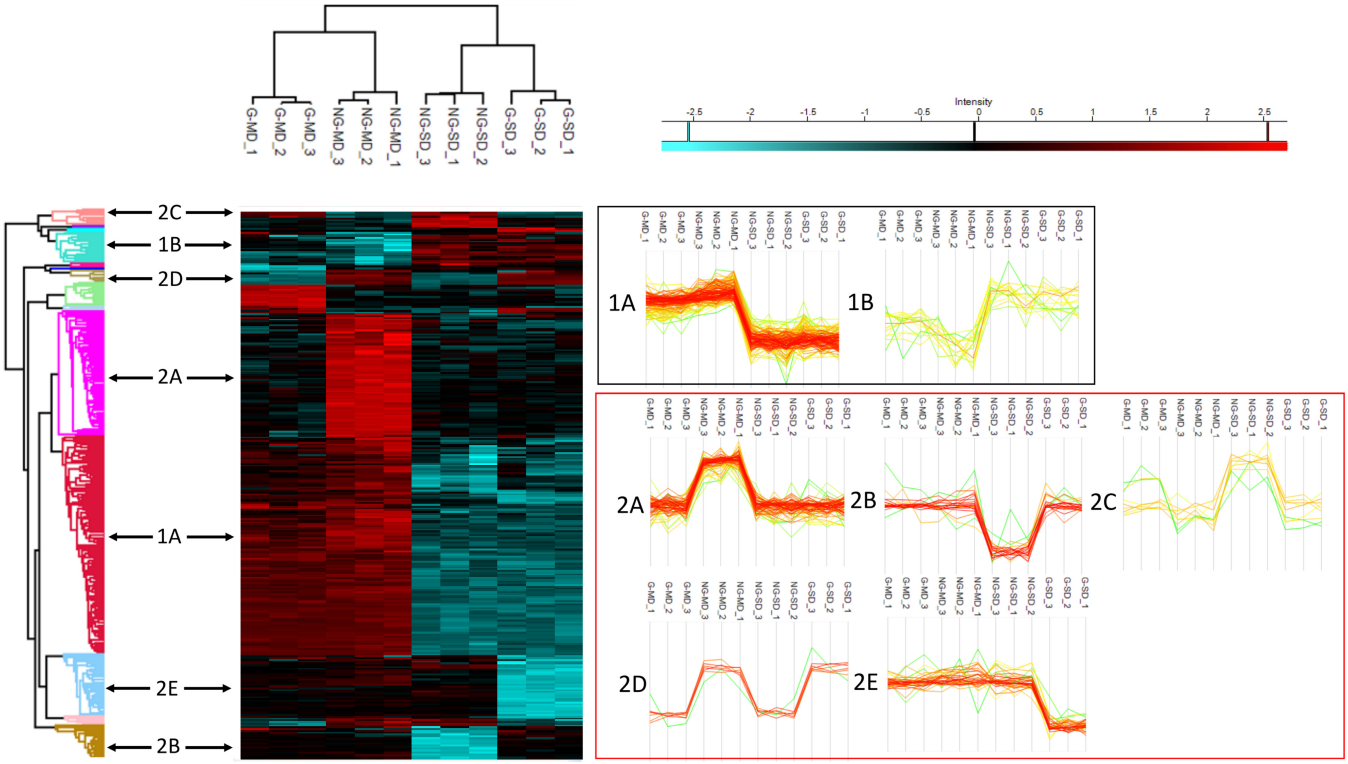

FIGURE 4 Hierarchical clustering and expression profiles of two-way ANOVA statistically significant proteins. The most interesting protein profiles are shown.

TABLE 2 Main severe drought-dependent DAPs involved in amino acid metabolism, protein metabolism, regulation of cell differentiation and proline degradation with their respective intensity values

Protein_ID	TAIR ID	Description	G-MD	NG-MD	NG-SD	G-SD	Cluster
Amino acid metabolism							
POPTR_0018s08910.1	AT5G19550.1	Aspartate aminotransferase 2	25.94	26.6	24.76	25.06	1A
POPTR_0003s07020.1	AT1G72330.1	Alanine aminotransferase 2	24.44	24.54	20.9	21.14	1A
POPTR_0019s05050.1	AT5G18170.1	Glutamate dehydrogenase 1	26.8	27.28	26	25.83	1A
POPTR_0002s14720.1	AT4G08900.1	Arginase	24.72	24	20.94	21.01	1A
POPTR_0002s24520.2	AT2G34470.1	Urease accessory protein G	25.62	25.47	21.02	21.2	1A
POPTR_0005s25100.1	AT1G75330.1	Ornithine carbamoyltransferase	23.9	24.71	21.26	20.85	1A
Protein metabolism							
POPTR_0005s25080.1	AT5G42790.1	Proteasome alpha subunit F1	25.59	25.54	21.32	21.29	1A
POPTR_0006s14260.1	AT2G05840.1	20S proteasome subunit PAA2	25.09	25.2	21.22	20.83	1A
POPTR_0001s16310.1	AT3G14290.1	20S proteasome alpha subunit E2	27.57	27.71	27.23	27.25	1A
POPTR_0014s18530.1	AT4G29040.1	Regulatory particle AAA-ATPase 2A	23.64	24.43	20.86	20.77	1A
POPTR_0014s15650.1	AT5G55160.1	Small ubiquitin-like modifier 2	25.12	25.31	21.31	21.25	1A
POPTR_0014s18530.1	AT4G29040.1	Regulatory particle AAA-ATPase 2A	23.64	24.43	20.86	20.77	1A
Regulation of cell differentiation							
POPTR_0009s02050.1	AT3G45600.1	Tetraspanin3	26.47	25.53	27.56	27.75	1B
POPTR_0009s11920.1	AT4G39260.3	Cold, circadian rhythm, and RNA binding 1	30.01	29.21	30.6	30.97	1B
Proline degradation							
POPTR_0015s07550.1	AT5G62530.1	Aldehyde dehydrogenase 12A1	24.5	24.81	20.98	21.28	1A

Note: Red shades correspond to the different intensity values of proteins.

TABLE 3 Main drought–girdling interaction-dependent DAPs involved in glycolytic process, lignin biosynthesis, cell wall biosynthesis and organization, ABA-signaling, ATP synthesis, proteasome and protein translation and belonging to clusters 2A, 2B, 2C, and 2D, with their respective intensity values.

Protein_ID	TAIR ID	Description	G-MD	NG-MD	NG-SD	G-SD	Cluster
Glycolytic process							
POPTR_0010s21100.1	AT3G55440.1	Triosephosphate isomerase	25.81	26.81	21.4	23.99	2B
POPTR_0008s08400.1	AT1G79550.2	Phosphoglycerate kinase	24.8	25.9	20.43	24.57	2B
Lignin biosynthesis							
POPTR_0006s03180.1	AT2G40890.1	Cytochrome P450, family 98, subfamily A	21.31	23.7	21.24	21.15	2A
POPTR_0012s00670.1	AT5G54160.1	*O*-methyltransferase 1	21.15	23.27	21.43	21.25	2A
POPTR_0011s15130.3	AT1G72680.1	Cinnamyl-alcohol dehydrogenase	20.99	24.03	21.15	21.62	2A
Cell wall biosynthesis and organization							
POPTR_0017s12760.1	AT3G29360.2	UDP-glucose 6-dehydrogenase family protein	21.03	25.16	21.18	21.44	2A
POPTR_0007s05490.1	AT5G65020.1	Annexin 2	21.28	25.28	21.08	21.59	2A
POPTR_0006s09610.1	AT5G23860.2	Tubulin beta 8	20.67	25.07	20.96	21	2A
POPTR_0001s46870.1	AT5G62690.1	Tubulin beta chain 2	20.93	23.02	21.29	21.17	2A
POPTR_0003s12000.1	AT1G63000.1	Nucleotide-rhamnose synthase/epimerase-reductase	20.85	23.63	21.15	21.12	2A
ABA-related							
POPTR_0010s19440.1	AT2G40170.1	Stress induced protein	24.88	21.19	24.93	21.25	2C
POPTR_0006s10480.1	AT5G01600.1	Ferretin 1	21.14	20.94	24.04	21.24	2C
ATP synthesis							
POPTR_0003s05880.1	AT1G80230.1	Rubredoxin-like superfamily protein	24.98	24.54	21.13	25.69	2B
POPTR_0015s06860.1	AT2G33040.1	Gamma subunit of Mt ATP synthase	24.79	25.58	21.27	23.52	2B
Protein translation							
POPTR_0006s25800.1	AT5G25757.1	RNA polymerase I-associated factor PAF67	25.81	25.79	21.46	25.61	2B
POPTR_0002s22460.1	AT4G02930.1	GTP binding Elongation factor Tu family protein	26.73	26.33	20.94	27.23	2B
POPTR_0010s22620.2	AT1G07930.1	GTP binding Elongation factor Tu family protein	21.33	25.04	21.71	24.77	2D
Proteasome							
POPTR_0015s15300.1	AT1G16470.1	Proteasome subunit PAB1	25.99	26.11	26.59	21.55	2E
POPTR_0008s17700.1	AT3G26340.1	Proteasome subunit beta type-5-B	25.40	25.54	25.44	21.35	2E
POPTR_0015s10280.1	AT4G24820.2	26S proteasome, regulatory subunit Rpn7	25.01	24.63	24.22	21.30	2E
POPTR_0008s14310.2	AT5G19990.1	26S proteasome regulatory subunit 8 homolog A	23.55	23.45	23.32	21.42	2E
POPTR_0014s03240.2	AT5G23540.1	26S proteasome non-ATPase regulatory subunit 14 homolog	25.71	25.93	24.78	21.61	2E
POPTR_0009s13620.1	AT5G66140.1	Proteasome alpha subunit D2	26.48	26.63	26.30	20.75	2E

Note: Red shades correspond to the different intensity values of proteins.

stress and girdling occurred. This proteomic alteration is the response to an impairment of the phloem transport independently of SD or girdling. These DAPs are mainly involved in primary metabolic processes such as the oxidative pentose phosphate pathway (transketolase and transaldolase), glycolysis, and nucleotide metabolism, as highlighted by ShinyGO enrichment analysis (Table S5). Moreover, some proteins are involved in lignin biosynthesis, such as POPTR_0006s03180.1 (a homolog of the cytochrome P450 enzyme 98A3), POPTR_0012s00670.1 (caffeic acid 3-*O*-methyltransferase [COMT] homolog), and POPTR_0011s15130.3 protein (cinnamyl alcohol dehydrogenase 1 [CAD1] homolog). Other enzymes are related to cell wall biosynthesis and organization, such as UDP-glucose 6-dehydrogenase (POPTR_0017s12760.1) and the nucleotide-rhamnose synthase/epimerase-reductase POPTR_0003s12000.1, or to cytoskeleton organization, such as the tubulins (POPTR_0006s09610.1, POPTR_0001s46870.1) and the annexin POPTR_0007s05490.1 (Table 3, Table S3).

The clusters 2B-E contain proteins whose abundance changed differently in NG and G seedlings if severely stressed (Figure 4; Table S4). These proteins represent the specific contribution of phloem flux to the fine root response to SD stress. The ATP metabolic process, the response to the metal ion and the proteasomal protein catabolism were some of the biological processes involving the proteins belonging to these clusters (Table S5). In particular, two enzymes

that play a central role in cytosolic glycolysis, the triose phosphate isomerase (TPI; POPTR_0010s21100.1) and the phosphoglycerate kinase (PGK3; POPTR_0008s08400.1), and two enzymes related to mitochondrial ATP synthesis-coupled proton transport, the cytochrome c oxidase subunit 5b-2 (POPTR_0003s05880.1) and the mitochondrial ATP synthase subunit gamma, (POPTR_0015s06860.1) decreased only in NG-SD seedlings (Table S4).

Other proteins more abundant in the very-fine roots of NG than G seedlings under SD included POPTR_0010s19440.1 and POPTR_0006s10480.1, homologs of the Em-like protein GEA6 (EM6) and ferritin1 (FER1) of Arabidopsis, respectively (Table S4). In particular, EM6 is a target of the ABA-responsive transcription factor ABI5. Interestingly, in Arabidopsis, the NF-YC9 protein mediates ABA signaling by interacting with ABI5 and facilitates the activation of the *EM6* gene promoter by ABI5 (Bi et al., 2017), which was detected only in the NG-SD seedlings. In addition, seven proteins involved in the proteasomal degradation and two proteins (Cystathionine beta-synthase [CBS] and copper/zinc superoxide dismutase) involved in cell redox homeostasis resulted less abundant in girdled seedlings upon SD (Table S5). Conversely, the Ras-related protein RABH1b homolog (POPTR_0003s08490.1), involved in protein transport, four proteins (POPTR_0010s22620.2, POPTR_0002s22460.1, POPTR_0006s25800, and POPTR_0005s05280.2) implicated in protein translation and the prohibitin 3 homolog (POPTR_0017s10480.2), a regulator for root development, were more abundant in G-SD seedlings.

4 | DISCUSSION

In this study, the interconnected morphological, physiological, chemical, and proteomic changes were investigated in the very fine roots of *F. sylvatica* seedlings in response to summer-related drought stress. Moreover, to explore the role of the starch reserves in coping with drought stress, the photosynthate flow from the shoots to roots was interrupted by the application of a girdling treatment.

4.1 | Morphological, physiological, and NSC responses to soil drying and plant girdling

Very-fine roots of control seedlings, that is, intact plants grown under the natural, moderate drought stress (NG-MD) condition, exhibited sigmoidal growth without significant root death in midsummer. This seasonal pattern of seedling growth differs from the bimodal growth pattern of adult beech trees reported in Southern Europe Mediterranean montane forests under similar drought conditions (Lozanova et al., 2019; Montagnoli et al., 2014). The sigmoidal seasonal pattern supports the findings of previous studies, which showed that drier soil conditions are needed for a significantly high death rate of seedling roots (Chiatante et al., 2006; Di Iorio et al., 2011; Espeleta & Eissenstat, 1998).

In spring, the marked growth of very-fine roots of control seedlings was accompanied by the accumulation of starch and SS, indicating higher resource availability and a strong downward push of new photosynthates into very-fine roots. On the other hand, in summer, the concentration of SS in very fine roots of control plants decreased much more (approximately −4%) than that of starch (approximately −1.5%), suggesting, in contrast to (Wiley et al., 2019), that SS are the main source of carbon, and that starch reserves, once refilled in springtime, are minimally used both during and after MD until autumn. Under the severe drought (NG-SD) condition, lower starch concentration and higher growth over NG-MD in September (Figure 1), that is, after the SD period, highlighted that very fine roots rely on their starch reserves to resume growth once the soil temperature and water content become adequate from end-August onward. Therefore, NG-SD seedlings consume their starch reserves 1 month earlier than NG-MD seedlings (Figures 2B and 3). The slight increase in the respiration rate of NG-SD plants in September correlated well with their resumed growth during that period. Respiration rates even higher than control have been observed in beech seedlings or saplings in drought release experiments but only when water was supplied in addition to rainfall (Di Iorio et al., 2016; Hagedorn et al., 2016). This starch reserve consumption could be attributed to impaired phloem loading in leaves and/or reduced transport velocity in sieve tubes (Hagedorn et al., 2016; Van Bel, 1990). Indeed, under MD conditions, the starch reserves appeared less available and rather sequestered (Sala et al., 2010), thus restraining plant growth even after the restoration of favorable soil conditions. A substantial difference between MD-treated plants and SD-treated seedlings is that the growth rate of the former was never zero and remained relatively constant throughout the experimental period, i.e., until the following spring (Figure 1).

The interruption of photosynthate supply in July from the shoot to roots of girdled plants exacerbated and anticipated by 1 further month the combined starch consumption-stimulated growth response (Figure 1), providing evidence for impaired phloem flux in intact beech seedlings under SD. The low respiration rate of girdled plants serves as evidence for the decline in metabolic activities due to carbon starvation; however, this reduction in respiration rate was less severe under MD, confirming the suppressive effect of prolonged drought stress on respiration (Huang et al., 2005, and references therein).

The decrease in water availability during the summer period is well known to determine an overall decrease in the photosynthetic rate and, consequently, in phloem loading. Sugars assimilated during the drought are involved in phloem osmotic adjustment as water becomes limiting, but turgor maintenance is possible only up to a limit, beyond which additional water stress causes a decrease in phloem turgor and transport rate (McDowell, 2011; Sala et al., 2010). Accordingly, in the very fine roots of NG-SD treated plants and all girdled plants, the constant decrease in SS content observed after July and the consequent loss of biomass between September and October may be explained by the required metabolic maintenance costs not balanced by the input of new photoassimilates via phloem flux.

The lack of difference in starch concentration between the taproot of moderately and severely drought-stressed seedlings suggests that phloem flux is not severely damaged up to the taproot but only in the peripheral portion of the root system, indicating that mortality

mechanisms under extreme drought are defined within individual compartments (leaves, branches, roots, etc.) rather than at the whole-organism level (Hartmann et al., 2013). On the other hand, girdling drastically reduced starch concentration in the taproot, suggesting that almost all starch reserves are mobilized to address the metabolic needs of the root system, regardless of water availability, and to support the reconstruction of the shoot. In fact, new sprouts produced below the girdle, which were immediately removed to avoid any supply of new photosynthates to the roots, further highlight the strong utilization of NSC reserves and girdling-induced breakage of apical dominance, similar to that reported in conifers (Wilson & Gartner, 2002) and aspen (Wan et al., 2006).

Consistent with the findings of Deng and colleagues (Deng et al., 2020), our results indicate that variation in NSCs tends to precede any variation in biomass partitioning, thus indicating that the distribution of biomass varies with NSC allocation under prolonged environmental stress.

4.2 | Phloem flux interruption modulates the molecular response of very fine roots to SD stress

The proteomic analysis provided insights into the molecular mechanisms underlying alterations in very fine roots during the driest period of the growing season. Moreover, the girdling approach enabled us to extrapolate the specific role of carbohydrate flux from the plant response to SD stress.

The abundance of many energy-metabolism-related enzymes decreased in the very fine roots of all SD stress-treated plants (intact and girdled), possibly to establish a new energy homeostasis. The main metabolic processes regulated by these enzymes included starch biosynthesis, glycolysis, and the TCA cycle (Table 2). It has been hypothesized that carbohydrate-degrading enzymes are downregulated under SD stress to slow down root starch mobilization because the accumulation of sugars facilitates fast recovery from drought stress (Di Iorio et al., 2016). This hypothesis is consistent with the maintenance of starch levels in NG-SD roots after 42 days of SD. In addition, the decrease in SS metabolism may contribute to the drought-induced osmotic protection.

SD negatively affects several enzymes related to amino acid metabolism, such as glutamate dehydrogenase, which participates in NH_4^+ assimilation. Reduction in the abundance of ornithine carbamoyltransferase could enhance the level of ornithine, a precursor of important compounds such as proline, which plays a central role in many metabolic pathways involved in abiotic stress resistance (Furlan et al., 2020; Kalamaki et al., 2009; Verslues & Sharma, 2010; Xue et al., 2009). These data, together with the decrease in the abundance of proteins such as δ-1-pyrroline-5-carboxylate dehydrogenase 12A1, which is involved in proline degradation (Table 2), indicate a possible involvement of proline.

On the other hand, our proteomic analysis suggested that the response of very fine roots to SD also depends on the impairment of phloem flux. In fact, several enzymes related to carbon metabolism, including some lignin biosynthesis-related enzymes (Table 3), showed a similar reduction in abundance in debarked and SD stress-treated intact plants. Sugars are not only metabolic resources but also structural constituents of cells. Roots with decreased lignin accumulation require less carbon per unit length, which may benefit plants by maintaining their root elongation capacity under decreased carbon flow to the roots. In addition, changes in the levels of various cell wall-related enzymes may result in the remodeling or loosening of the cell wall (Reboul et al., 2011). Overall, these data support, at least in part, the significant increase in the length, but not in the dry weight, of very fine roots after stem girdling and the preservation of root growth in intact plants after 42 days of SD stress (Figure 1). An increase in the length of very fine roots has also been proposed as a critical feature used by plants to acquire water under drought-stress conditions (Canales et al., 2019; Wasson et al., 2012). The higher levels of several stress-related proteins, such as Arabidopsis FER1, EM6, and NF-YC9 homologs, in NG-SD than in G-SD seedlings indicate that the SD tolerance of very fine roots depends, at least in part, on the phloem transport. Moreover, SD stress-induced reduction in the abundance of several proteasome subunits in girdled plants suggests an imbalance in the ubiquitin-dependent proteolytic pathway (Table 3; Table S4). A reduction in proteasome activity is expected to decrease the capacity of cells to remove misfolded proteins, resulting in the accumulation and aggregation of these proteins, which can accelerate cell death (Kurepa et al., 2008). Reduction in the abundance of a copper/zinc superoxide dismutase and a cystathionine β-synthase (Table S4), both involved in cell redox homeostasis, in G-SD seedlings also highlights the importance of phloem flux for coping with SD stress. Conversely, protein translation and glycolysis-related proteins, as well as prohibitin 3 homolog, which is involved in meristematic cell proliferation (Huang et al., 2019), were more abundant in the very fine roots of G-SD seedlings than in those of NG-SD seedlings (Table 3; Table S4). This result may be related to the greater increase in the root length of girdled seedlings upon SD until the fast depletion of storage reserves.

5 | CONCLUSION

Ongoing climate change is expected to substantially increase temperature and alter precipitation patterns globally. Tree roots react to drought stress by implementing a variety of strategies to avoid and tolerate potential damage.

Overall, our results showed that the mobilization of starch reserves in the very fine roots of *F. sylvatica* seedlings during the period of SD was not as high as that after the drought when favorable conditions of soil temperature and water content were restored at the end of the summer season. This moment coincides with a new flush of growth, albeit to a lesser extent than that observed in the spring. The interruption of phloem flux resulting from the girdling treatment highlights how the physiological responses of very fine roots to SD stress are closely related to the flux of photosynthates from the shoot to the root system and how the consequent changes in NSC allocation alter the distribution of biomass.

Here, *for the first time*, molecular mechanisms underlying the responses of very fine roots to SD were investigated for extrapolating the responses that depend on the reduction of phloem transport. Proteomic analysis performed at the end of the driest period of the growing season supported the physiological data. Indeed, it showed that the very fine roots of all SD stress-treated plants (intact and girdled) underwent molecular remodeling, which decreased the abundance of carbon metabolism-related enzymes and thus slowed down the consumption of energy resources. Moreover, a reconfiguration of amino acid metabolism facilitated the maintenance of osmotic potential. On the other hand, the response of NG-SD very fine roots to SD stress involved the regulation of enzymes required for cell wall remodeling and stress response.

In conclusion, this study revealed a new view of the multifaceted response of very fine roots of *F. sylvatica* seedlings to SD, revealing phloem flux as a key factor controlling carbohydrate metabolism.

AUTHOR CONTRIBUTIONS

Antonino Di Iorio and Candida Vannini conceived and contributed respectively to the experimental design; Antonino Di Iorio, Guido Domingo, Elena Costantini, Milena Marsoni, and Federica Mulè performed the experiments, and all authors analyzed and interpreted the data. Antonino Di Iorio, Guido Domingo, and Candida Vannini wrote the original draft, and all authors contributed to review and editing.

ACKNOWLEDGMENTS

We are deeply grateful to Federica Mulè for her valuable help in the laboratory analyses, and the Functional Genomics Center Zurich (ETH, Zurich) for Label-free protein quantification. This work was supported by the University of Insubria (FAR).

CONFLICT OF INTEREST STATEMENT

The authors declare that they have no conflict of interest.

DATA AVAILABILITY STATEMENT

All data supporting the findings of this study are available within the article and within its supporting information published online. All raw data, databases, and processing parameters are available on ProteomeXchange via PRIDE repository.

ORCID

Guido Domingo https://orcid.org/0000-0002-2617-8873

REFERENCES

Abu-Hamdeh, N.H. & Reeder, R.C. (2000) Soil thermal conductivity effects of density, moisture, salt concentration, and organic matter. *Soil Science Society of America Journal*, 64(4), 1285–1290. Available from: https://doi.org/10.2136/sssaj2000.6441285x

Atkin, O.K. & Tjoelker, M.G. (2003) Thermal acclimation and the dynamic response of plant respiration to temperature. *Trends in Plant Science*, 8(7), 343–351.

Bi, C., Ma, Y., Wang, X.-F. & Zhang, D.-P. (2017) Overexpression of the transcription factor NF-YC9 confers abscisic acid hypersensitivity in Arabidopsis. *Plant Molecular Biology*, 95(4), 425–439.

Bouma, T.J., Nielsen, K.L., Eissenstat, D.M. & Lynch, J.P. (1997) Estimating respiration of roots in soil: interactions with soil CO_2, soil temperature and soil water content. *Plant and Soil*, 195(2), 221–232.

Brunner, I., Herzog, C., Dawes, M.A., Arend, M. & Sperisen, C. (2015) How tree roots respond to drought. *Frontiers in Plant Science*, 6, 547.

Burton, A.J., Pregitzer, K.S., Zogg, G.P. & Zak, D.R. (1996) Latitudinal variation in sugar maple fine root respiration. *Canadian Journal of Forest Research*, 26(10), 1761–1768.

Canales, F.J., Nagel, K.A., Müller, C., Rispail, N. & Prats, E. (2019) Deciphering root architectural traits involved to cope with water deficit in oat. *Frontiers in Plant Science*, 10, 1558.

Chiatante, D., Iorio, A.D., Sciandra, S., Scippa, G.S. & Mazzoleni, S. (2006) Effect of drought and fire on root development in Quercus pubescens Willd. and Fraxinus ornus L. seedlings. *Environmental and Experimental Botany*, 56(2), 190–197.

Cullotta, S., Puzzolo, V. & Fresta, A. (2015) The southernmost beech (Fagus sylvatica) forests of Europe (Mount Etna, Italy): ecology, structural stand-type diversity and management implications. *Plant Biosystems*, 149(1), 88–99.

Cuneo, I.F., Knipfer, T., Brodersen, C.R. & McElrone, A.J. (2016) Mechanical failure of fine root cortical cells initiates plant hydraulic decline during drought. *Plant Physiology*, 172(3), 1669–1678.

Deng, X., Xiao, W., Shi, Z., Zeng, L. & Lei, L. (2020) Combined effects of drought and shading on growth and non-structural carbohydrates in *Pinus massoniana* lamb seedlings. *Forests*, 11(1), 18.

Di Iorio, A., Giacomuzzi, V. & Chiatante, D. (2016) Acclimation of fine root respiration to soil warming involves starch deposition in very fine and fine roots: a case study in Fagus sylvatica saplings. *Physiologia Plantarum*, 156(3), 294–310.

Di Iorio, A., Montagnoli, A., Scippa, G.S. & Chiatante, D. (2011) Fine root growth of *Quercus pubescens* seedlings after drought stress and fire disturbance. *Environmental and Experimental Botany*, 74, 272–279.

Ellenberg, H. (1988) *Vegetation ecology of Central Europe*, 4th edition. Cambridge: Cambridge University Press.

Espeleta, J.F. & Eissenstat, D.M. (1998) Responses of citrus fine roots to localized soil drying: a comparison of seedlings with adult fruiting trees. *Tree Physiology*, 18(2), 113–119.

Foley, S.W., Gosai, S.J., Wang, D., Selamoglu, N., Sollitti, A.C., Köster, T. et al. (2017) A global view of RNA-protein interactions identifies post-transcriptional regulators of root hair cell fate. *Developmental Cell*, 41(2), 204–220.e205.

Fotelli, M.N., Nahm, M., Radoglou, K., Rennenberg, H., Halyvopoulos, G. & Matzarakis, A. (2009) Seasonal and interannual ecophysiological responses of beech (Fagus sylvatica) at its south-eastern distribution limit in Europe. *Forest Ecology and Management*, 257(3), 1157–1164.

Furlan, A.L., Bianucci, E., Giordano, W., Castro, S. & Becker, D.F. (2020) Proline metabolic dynamics and implications in drought tolerance of peanut plants. *Plant Physiology and Biochemistry*, 151, 566–578.

Galvez, D.A., Landhäusser, S.M. & Tyree, M.T. (2013) Low root reserve accumulation during drought may lead to winter mortality in poplar seedlings. *The New Phytologist*, 198(1), 139–148.

Ge, S.X., Jung, D. & Yao, R. (2020) ShinyGO: a graphical gene-set enrichment tool for animals and plants. *Bioinformatics*, 36(8), 2628–2629.

Geilfus, C.-M., Carpentier, S.C., Zavišić, A. & Polle, A. (2017) Changes in the fine root proteome of Fagus sylvatica L. trees associated with P-deficiency and amelioration of P-deficiency. *Journal of Proteomics*, 169, 33–40.

Geßler, A., Keitel, C., Kreuzwieser, J., Matyssek, R., Seiler, W. & Rennenberg, H. (2007) Potential risks for European beech (Fagus sylvatica L.) in a changing climate. *Trees*, 21(1), 1–11.

Guo, D., Xia, M., Wei, X., Chang, W., Liu, Y. & Wang, Z. (2008) Anatomical traits associated with absorption and mycorrhizal colonization are linked to root branch order in twenty-three Chinese temperate tree species. *The New Phytologist*, 180(3), 673–683.

Gupta, S., Mishra, S.K., Misra, S., Pandey, V., Agrawal, L., Nautiyal, C.S. et al. (2020) Revealing the complexity of protein abundance in chickpea root under drought-stress using a comparative proteomics approach. *Plant Physiology and Biochemistry*, 151, 88–102.

Hagedorn, F., Joseph, J., Peter, M., Luster, J., Pritsch, K., Geppert, U. et al. (2016) Recovery of trees from drought depends on belowground sink control. *Nature Plants*, 2(8), 16111.

Hartmann, H., Moura, C.F., Anderegg, W.R.L., Ruehr, N.K., Salmon, Y., Allen, C.D. et al. (2018) Research frontiers for improving our understanding of drought-induced tree and forest mortality. *New Phytologist*, 218(1), 15–28. Available from: https://doi.org/10.1111/nph.15048

Hartmann, H., Ziegler, W., Kolle, O. & Trumbore, S. (2013) Thirst beats hunger – declining hydration during drought prevents carbon starvation in Norway spruce saplings. *New Phytologist*, 200(2), 340–349. Available from: https://doi.org/10.1111/nph.12331

Huang, R., Yang, C. & Zhang, S. (2019) The Arabidopsis PHB3 is a pleiotropic regulator for plant development. *Plant Signaling & Behavior*, 14(11), 1656036.

Huang, X., Lakso, A.N. & Eissenstat, D.M. (2005) Interactive effects of soil temperature and moisture on Concord grape root respiration. *Journal of Experimental Botany*, 56(420), 2651–2660.

Jackson, R.B., Mooney, H.A. & Schulze, E.D. (1997) A global budget for fine root biomass, surface area, and nutrient contents. *Proceedings of the National Academy of Sciences of the United States of America*, 94(14), 7362–7366.

Jia, S., McLaughlin, N.B., Gu, J., Li, X. & Wang, Z. (2013) Relationships between root respiration rate and root morphology, chemistry and anatomy in Larix gmelinii and Fraxinus mandshurica. *Tree Physiology*, 33(6), 579–589.

Kalamaki, M.S., Merkouropoulos, G. & Kanellis, A.K. (2009) Can ornithine accumulation modulate abiotic stress tolerance in Arabidopsis? *Plant Signaling & Behavior*, 4(11), 1099–1101.

Kurepa, J., Toh-E, A. & Smalle, J.A. (2008) 26S proteasome regulatory particle mutants have increased oxidative stress tolerance. *The Plant Journal*, 53(1), 102–114.

Landhäusser, S.M., Chow, P.S., Dickman, L.T., Furze, M.E., Kuhlman, I., Schmid, S. et al. (2018) Standardized protocols and procedures can precisely and accurately quantify non-structural carbohydrates. *Tree Physiology*, 38(12), 1764–1778.

Li, C.Y., Weiss, D. & Goldschmidt, E.E. (2003) Girdling affects carbohydrate-related gene expression in leaves, bark and roots of alternate-bearing citrus trees. *Annals of Botany*, 92(1), 137–143.

Li, H., Li, Y., Ke, Q., Kwak, S.-S., Zhang, S. & Deng, X. (2020) Physiological and differential proteomic analyses of imitation drought stress response in Sorghum bicolor root at the seedling stage. *International Journal of Molecular Sciences*, 21(23), 9174.

Li, Y., Zhang, W., Zhang, D., Zheng, Y., Xu, Y., Liu, B. et al. (2022) Mechanism of [CO_2] enrichment alleviated drought stress in the roots of cucumber seedlings revealed via proteomic and biochemical analysis. *International Journal of Molecular Sciences*, 23(23), 14911.

Lipp, C.C. & Andersen, C.P. (2003) Role of carbohydrate supply in white and brown root respiration of ponderosa pine. *The New Phytologist*, 160(3), 523–531.

Liu, H., Sultan, M.A.R.F., Xl, L., Zhang, J., Yu, F. & Hx, Z. (2015) Physiological and comparative proteomic analysis reveals different drought responses in roots and leaves of drought-tolerant wild wheat (Triticum boeoticum). *PLoS One*, 10(4), e0121852.

Liu, Y., Ji, D., Turgeon, R., Chen, J., Lin, T., Huang, J. et al. (2019) Physiological and proteomic responses of mulberry trees (Morus alba. L.) to combined salt and drought stress. *International Journal of Molecular Sciences*, 10(4), 2486.

Lozanova, L., Zhiyanski, M., Vanguelova, E., Doncheva, S., Marinov, M.P. & Lazarova, S. (2019) Dynamics and vertical distribution of roots in European beech forests and Douglas fir plantations in Bulgaria. *Forests*, 10(12), 1123.

Makita, N., Hirano, Y., Dannoura, M., Kominami, Y., Mizoguchi, T., Ishii, H. et al. (2009) Fine root morphological traits determine variation in root respiration of Quercus serrata. *Tree Physiology*, 29(4), 579–585.

Makita, N., Hirano, Y., Mizoguchi, T., Kominami, Y., Dannoura, M., Ishii, H. et al. (2011) Very fine roots respond to soil depth: biomass allocation, morphology, and physiology in a broad-leaved temperate forest. *Ecological Research*, 26(1), 95–104. Available from: https://doi.org/10.1007/s11284-010-0764-5

McCormack, M.L., Dickie, I.A., Eissenstat, D.M., Fahey, T.J., Fernandez, C.W., Guo, D. et al. (2015) Redefining fine roots improves understanding of below-ground contributions to terrestrial biosphere processes. *New Phytologist*, 207(3), 505–518. Available from: https://doi.org/10.1111/nph.13363

McDowell, N., Pockman, W.T., Allen, C.D., Breshears, D.D., Cobb, N., Kolb, T. et al. (2008) Mechanisms of plant survival and mortality during drought: why do some plants survive while others succumb to drought? *New Phytologist*, 178(4), 719–739. Available from: https://doi.org/10.1111/j.1469-8137.2008.02436.x

McDowell, N.G. (2011) Mechanisms linking drought, hydraulics, carbon metabolism, and vegetation mortality. *Plant Physiology*, 155(3), 1051–1059.

Montagnoli, A., Di Iorio, A., Terzaghi, M., Trupiano, D., Scippa, G.S. & Chiatante, D. (2014) Influence of soil temperature and water content on fine-root seasonal growth of European beech natural forest in southern Alps, Italy. *European Journal of Forest Research*, 133(5), 957–968.

Montagnoli, A., Dumroese, R.K., Terzaghi, M., Onelli, E., Scippa, G.S. & Chiatante, D. (2019) Seasonality of fine root dynamics and activity of root and shoot vascular cambium in a Quercus ilex L. forest (Italy). *Forest Ecology and Management*, 431, 26–34.

Montagnoli, A., Terzaghi, M., Di Iorio, A., Scippa, G.S. & Chiatante, D. (2012) Fine-root seasonal pattern, production and turnover rate of European beech (Fagus sylvatica L.) stands in Italy Prealps: possible implications of coppice conversion to high forest. *Plant Biosystems*, 146(4), 1012–1022.

Oberhuber, W., Gruber, A., Lethaus, G., Winkler, A. & Wieser, G. (2017) Stem girdling indicates prioritized carbon allocation to the root system at the expense of radial stem growth in Norway spruce under drought conditions. *Environmental and Experimental Botany*, 138, 109–118.

Palta, J.A. & Nobel, P.S. (1989) Influences of water status, temperature, and root age on daily patterns of root respiration for two cactus species. *Annals of Botany*, 63(6), 651–662.

Paradiso, A., Domingo, G., Blanco, E., Buscaglia, A., Fortunato, S., Marsoni, M. et al. (2020) Cyclic AMP mediates heat stress response by the control of redox homeostasis and ubiquitin-proteasome system. *Plant, Cell & Environment*, 43(11), 2727–2742. Available from: https://doi.org/10.1111/pce.13878

Perez-Riverol, Y., Csordas, A., Bai, J., Bernal-Llinares, M., Hewapathirana, S., Kundu, D.J. et al. (2019) The PRIDE database and related tools and resources in 2019: improving support for quantification data. *Nucleic Acids Research*, 47(D1), D442–D450.

Polverigiani, S., McCormack, M.L., Mueller, C.W. & Eissenstat, D.M. (2011) Growth and physiology of olive pioneer and fibrous roots exposed to soil moisture deficits. *Tree Physiology*, 31(11), 1228–1237.

Reboul, R., Geserick, C., Pabst, M., Frey, B., Wittmann, D., Lütz-Meindl, U. et al. (2011) Down-regulation of UDP-glucuronic acid biosynthesis leads to swollen plant cell walls and severe developmental defects associated with changes in pectic polysaccharides. *The Journal of Biological Chemistry*, 286(46), 39982–39992.

Sala, A., Piper, F. & Hoch, G. (2010) Physiological mechanisms of drought-induced tree mortality are far from being resolved. *The New Phytologist*, 186(2), 274–281.

Schall, P., Lödige, C., Beck, M. & Ammer, C. (2012) Biomass allocation to roots and shoots is more sensitive to shade and drought in European beech than in Norway spruce seedlings. *Forest Ecology and Management*, 266, 246–253.

Ueda, M., Matsui, K., Ishiguro, S., Sano, R., Wada, T., Paponov, I. et al. (2004) The HALTED ROOT gene encoding the 26S proteasome subunit RPT2a is essential for the maintenance of Arabidopsis meristems. *Development*, 131(9), 2101–2111.

Van Bel, A.J.E. (1990) Xylem—phloem exchange via the rays: the undervalued route of transport. *Journal of Experimental Botany*, 41(227), 631–644.

Vannini, C., Domingo, G., Fiorilli, V., Seco, D.G., Novero, M., Marsoni, M. et al. (2021) Proteomic analysis reveals how pairing of a Mycorrhizal fungus with plant growth-promoting bacteria modulates growth and defense in wheat. *Plant, Cell & Environment*, 44(6), 1946–1960. Available from: https://doi.org/10.1111/pce.14039

Vannini, C., Marsoni, M., Scoccianti, V., Ceccarini, C., Domingo, G., Bracale, M. et al. (2019) Proteasome-mediated remodeling of the proteome and phosphoproteome during kiwifruit pollen germination. *Journal of Proteomics*, 192, 334–345.

Vartanian, N. & Chauveau, M. (1986) Etude in vitro de la reprise de la respiration racinaire chez la Moutarde et le Colza après une période de sécheresse/In vitro study of root respiration recovery following a drought stress period. *Plant and Soil*, 92(2), 255–264.

Verslues, P.E. & Sharma, S. (2010) Proline metabolism and its implications for plant-environment interaction. *Arabidopsis Book*, 8, e0140.

Vogel, C. & Marcotte, E.M. (2012) Insights into the regulation of protein abundance from proteomic and transcriptomic analyses. *Nature Reviews. Genetics*, 13(4), 227–232.

Wan, X., Landhäusser, S.M., Lieffers, V.J. & Zwiazek, J.J. (2006) Signals controlling root suckering and adventitious shoot formation in aspen (Populus tremuloides). *Tree Physiology*, 26(5), 681–687.

Wang, C., Brunner, I., Zong, S. & Li, M.-H. (2019) The dynamics of living and dead fine roots of Forest biomes across the northern hemisphere. *Forests*, 10(11), 953.

Wang, F., Muto, A., Van de Velde, J., Neyt, P., Himanen, K., Vandepoele, K. et al. (2015) Functional analysis of the Arabidopsis TETRASPANIN gene family in plant growth and development. *Plant Physiology*, 169(3), 2200–2214.

Wasson, A.P., Richards, R.A., Chatrath, R., Misra, S.C., Prasad, S.V., Rebetzke, G.J. et al. (2012) Traits and selection strategies to improve root systems and water uptake in water-limited wheat crops. *Journal of Experimental Botany*, 63(9), 3485–3498.

Wiant, H.V. (1967) Contribution of roots to forest soil respiration. *Advanced Frontiers in Plant Science*, 18, 163–167.

Wiley, E., King, C.M. & Landhäusser, S.M. (2019) Identifying the relevant carbohydrate storage pools available for remobilization in aspen roots. *Tree Physiology*, 39(7), 1109–1120.

Wilson, B.F. & Gartner, B.L. (2002) Effects of phloem girdling in conifers on apical control of branches, growth allocation and air in wood. *Tree Physiology*, 22(5), 347–353.

Xiao, S., Liu, L., Zhang, Y., Sun, H., Zhang, K., Bai, Z. et al. (2020) Tandem mass tag-based (TMT) quantitative proteomics analysis reveals the response of fine roots to drought stress in cotton (Gossypium hirsutum L.). *BMC Plant Biology*, 20(1), 328.

Xue, X., Liu, A. & Hua, X. (2009) Proline accumulation and transcriptional regulation of proline biosynthesis and degradation in Brassica napus. *BMB Reports*, 42(1), 28–34.

SUPPORTING INFORMATION

Additional supporting information can be found online in the Supporting Information section at the end of this article.

How to cite this article: Domingo, G., Vannini, C., Marsoni, M., Costantini, E., Bracale, M. & Di Iorio, A. (2023) A multifaceted approach to reveal the very-fine root's response of *Fagus sylvatica* seedlings to different drought intensities. *Physiologia Plantarum*, 175(3), e13934. Available from: https://doi.org/10.1111/ppl.13934